J. Non-Newtonian Fluid Mech. 165 (2010) 544–550

Contents lists available at ScienceDirect

Journal of Non-Newtonian Fluid Mechanics

journal homepage: www.elsevier.com/locate/jnnfm

Short communication

Numerical simulations of cessation flows of a Bingham plastic with the augmented Lagrangian method

Larisa Muravleva[a], Ekaterina Muravleva[b], Georgios C. Georgiou[c], Evan Mitsoulis[d,*]

[a] Department of Mechanics and Mathematics, Lomonosov Moscow State University, 119991, Moscow, Russia
[b] Institute of Numerical Mathematics, Russian Academy of Sciences, 119333, Moscow, Russia
[c] Department of Mathematics and Statistics, University of Cyprus, P.O. Box 20537, 1678, Nicosia, Cyprus
[d] School of Mining Engineering & Metallurgy, National Technical University of Athens, Zografou, 15780, Athens, Greece

ARTICLE INFO

Article history:
Received 23 December 2009
Received in revised form 29 January 2010
Accepted 2 February 2010

Keywords:
Bingham plastic
Poiseuille flows
Variational inequalities
Augmented Lagrangian method (ALM)
Iterative Uzawa algorithm
Cessation flows
Finite stopping times

ABSTRACT

The augmented Lagrangian/Uzawa method has been used to study benchmark one-dimensional cessation flow problems of a Bingham fluid, such as the plane Couette flow, and the plane, round, and annular Poiseuille flows. The calculated stopping times agree well with available theoretical upper bounds for the whole range of Bingham numbers and with previous numerical results. The applied method allows for easy determination of the yielded and unyielded regions. The evolution of the rigid zones in these unsteady flows is presented. It is demonstrated that the appearance of an unyielded zone near the wall occurs for any non-zero Bingham number not only in the case of a round tube but also in the case of an annular tube of small radii ratio. The advantages of using the present method instead of regularizing the constitutive equation are also discussed.

1. Introduction

Recently, Chatzimina et al. [1,2] solved numerically several one-dimensional cessation flows of a Bingham plastic, i.e. the plane Couette flow [1], and the plane, round, and annular Poiseuille flows [1,2], in order to compare the numerical stopping times with the theoretical upper bounds obtained by Glowinski [3] and Huilgol et al. [4] and study the evolution of the yielded/unyielded regions. The inherent discontinuity of the ideal Bingham plastic model was overcome by using Papanastasiou's exponential regularization [5]. This model gives an accurate representation of the ideal Bingham model when the stress-growth regularization parameter approaches infinity [5,6]. The numerical results in Refs. [1,2] have been mostly obtained for relatively low values of the regularization parameter, which lead to satisfactory estimates of the stopping times only for moderate and high values of the Bingham number, which is a measure of the fluid yield stress. Chatzimina et al. [1,2] pointed out that in order to improve the accuracy of the calculated stopping times at low and moderate Bingham numbers, the regularization parameter should be increased to values that lead to prohibitively very long computation times for such time-dependent calculations.

Regularization methods may offer an attractive alternative to the ideal Bingham model [7] for engineering calculations, but may also mask interesting viscoplastic effects. It has been convincingly argued that variational inequalities [3,8] are better suited for obtaining accurate results for the yielded/unyielded zones and finite stopping times when using the ideal Bingham model or its variants (Herschel–Bulkley and Casson models). The method of choice for solving these problems is the augmented Lagrangian method (ALM) with an Uzawa-like iteration.

Two slightly different numerical implementations of the method have been proposed. In the first version, suggested originally for steady-state Poiseuille flows [9], only one tensor (Lagrange multiplier) is additionally introduced. This method is discussed in a recent review by Dean et al. [10]. More complicated cases based on this method have also been published [11–13]. In the second version, two tensors (Lagrange multiplier and independent rate-of-strain tensor) are introduced. This augmented Lagrangian method introduced by Fortin and Glowinski [14] has been widely used during the last years. An early example is the work by Huilgol and Panizza [15]. The method has been applied for steady pipe flows [16–22] and for some two-dimensional problems [23–25].

The objective of the present work is to compare the performance and the results of the former method to the regularized time-dependent 1D results of Chatzimina et al. [1,2], in view of the existing theoretical upper bounds of Glowinski [3] and Huilgol et al. [4]. The emphasis will be on showing the numerical stopping

* Corresponding author.
E-mail address: mitsouli@metal.ntua.gr (E. Mitsoulis).

0377-0257/$ – see front matter © 2010 Elsevier B.V. All rights reserved.
doi:10.1016/j.jnnfm.2010.02.002

times by the two methods and the evolution of yielded/unyielded regions. Conclusions will be drawn about the advantages of each method to handle viscoplastic problems.

2. Problem statement and method of solution

We have studied four cessation flows of a Bingham plastic: (a) plane Couette flow; (b) plane Poiseuille flow; (c) axisymmetric Poiseuille flow; and (d) annular Poiseuille flow. The problems at hand are made dimensionless using the same scales as those used in Chatzimina et al. [1,2]: the lengths are scaled by a characteristic length, L, and the velocity is scaled by a characteristic velocity, U. Then the time is scaled by $\rho L^2/\mu$ (ρ being the density and μ the viscosity), and the pressure and stress are scaled by $\mu U/L$. In the case of the plane Couette flow, L is the gap size H and U is the initial speed of the moving upper plate. The characteristic length is the channel half-width, H, in the case of the plane Poiseuille flow, the radius, R, of the tube in the case of axisymmetric Poiseuille flow, and the radius of the outer cylinder in the case of the annular Poiseuille flow. In the case of Poiseuille flows, U is the initial average velocity.

With the above non-dimensionalization the constitutive equation for a Bingham fluid becomes

$$\left.\begin{array}{ll} \dot{\boldsymbol{\gamma}} = \mathbf{0}, & |\boldsymbol{\tau}| \le Bn \\ \boldsymbol{\tau} = \left(1 + \dfrac{Bn}{|\dot{\boldsymbol{\gamma}}|}\right)\dot{\boldsymbol{\gamma}}, & |\boldsymbol{\tau}| > Bn \end{array}\right\}, \tag{1}$$

where $\boldsymbol{\tau}$ is the stress tensor and $\dot{\boldsymbol{\gamma}} \equiv \nabla \boldsymbol{u} + (\nabla \boldsymbol{u})^{\boldsymbol{T}}$ is the rate-of-strain tensor (all dimensionless), while $|\dot{\boldsymbol{\gamma}}|$ and $|\boldsymbol{\tau}|$ denote the magnitudes of the corresponding tensors. For example,

$$|\dot{\boldsymbol{\gamma}}| = \sqrt{\frac{1}{2} II_{\dot{\boldsymbol{\gamma}}}} = \left[\frac{1}{2}\{\dot{\boldsymbol{\gamma}} : \dot{\boldsymbol{\gamma}}\}\right]^{1/2}, \tag{2}$$

where $II_{\dot{\boldsymbol{\gamma}}}$ is the second invariant of $\dot{\boldsymbol{\gamma}}$.

In Eq. (1), Bn denotes the Bingham number, which is defined as follows

$$Bn = \frac{\tau_0 L}{\mu U}, \tag{3}$$

with τ_0 being the yield stress. Another dimensionless number appears in the case of the annular Poiseuille flow; this is the radii ratio, $k \equiv R_1/R_2$ with $0 < k < 1$.

As an example, we consider the time-dependent, unidirectional, one-dimensional plane Poiseuille flow (the axisymmetric problems can be similarly formulated). We assume that the only non-zero-velocity component is in the z-direction: $\boldsymbol{u} = (0, 0, u(y, t))$. At time $t = 0$ the velocity $u^0(y, 0) = u_0(y)$. A no-slip condition is imposed at the two plates: $u(-1) = u(1) = 0$. Thus, the dimensionless momentum equation is reduced to:

$$\frac{\partial u}{\partial t} = \frac{\partial \tau}{\partial y} + C(t), \tag{4}$$

where $\tau \equiv \tau_{yz}$ is defined by Eq. (1) and $C(t)$ is the dimensionless pressure gradient, which is time-dependent. For the time discretization, we used the standard fully-implicit backward Euler scheme. This scheme reads as follows: with the initial condition $u^0 = u_0$ and for $n \ge 1$, compute u^n from u^{n-1} via the solution of the minimization problem [26]

$$J(u^n) = \min_{\upsilon \in H_0^1(\Omega)} J(\upsilon), \tag{5}$$

where

$$J(\upsilon) = \frac{1}{2\Delta t}\int_\Omega \upsilon^2 dy + \frac{1}{2}\int_\Omega \left(\frac{\partial \upsilon}{\partial y}\right)^2 dy + Bn\int_\Omega \left|\frac{\partial \upsilon}{\partial y}\right| dy - \int_\Omega f\upsilon dy. \tag{6}$$

Δt is the time step and

$$f = \left(\frac{1}{\Delta t}\right) u^{n-1} + C(n\Delta t). \tag{7}$$

Accordingly [8], a scalar function λ exists such that

$$\tau = \frac{\partial u}{\partial y} + Bn\lambda, \quad \lambda\frac{\partial u}{\partial y} = \left|\frac{\partial u}{\partial y}\right|, \quad |\lambda| \le 1. \tag{8}$$

This expression holds everywhere in Ω (this includes the rigid region, i.e. where $\partial u/\partial y = 0$). We define the convex set of scalar functions: $\Lambda = \{q | q \in (L^2(\Omega)), \quad |q| \le 1\}$. The original minimization problem (5) corresponds to finding a saddle point of the Lagrangian functional $L : H_0^1(\Omega) \times \Lambda \to \mathbb{R}$ by [3,9]

$$L(\upsilon, q) = \frac{1}{2\Delta t}\int_\Omega \upsilon^2 dy + \frac{1}{2}\int_\Omega \left(\frac{\partial \upsilon}{\partial y}\right)^2 dy + Bn\int_\Omega q\frac{\partial \upsilon}{\partial y} dy - \int_\Omega f\upsilon dy. \tag{9}$$

We use the following notations: u^n, λ^n solution on the n time step problem. The solution algorithm can be written as follows:

1. Initialization of $u^0 = u_0(y)$.
2. For $n \ge 1$ and time loop $t = n\Delta t$, solve the viscoplastic problem by an Uzawa algorithm, as follows:

- Initialization of $\lambda_0^n = \lambda^{n-1}$.
- For $i \ge 1$, assuming that u^{n-1}, λ_{i-1}^n is known, compute u_i^n and λ_i^n by solving

$$\frac{u_i^n}{\Delta t} - \frac{\partial^2 u_i^n}{\partial y^2} = Bn\frac{\partial \lambda_{i-1}^n}{\partial y} + \frac{u^{n-1}}{\Delta t} + C(t^n), \quad u_i^n(0) = u_i^n(1) = 0, \tag{10}$$

- Compute the viscoplastic Lagrange multiplier, λ_i^n:

$$\lambda_i^n = \begin{cases} \lambda_{i-1}^n + rBn\dfrac{\partial u_i^n}{\partial y}, & \text{if } \left|\lambda_{i-1}^n + rBn\dfrac{\partial u_i^n}{\partial y}\right| < 1, \\ \dfrac{\lambda_{i-1}^n + rBn\dfrac{\partial u_i^n}{\partial y}}{\left|\lambda_{i-1}^n + rBn\dfrac{\partial u_i^n}{\partial y}\right|} & \text{if } \left|\lambda_{i-1}^n + rBn\dfrac{\partial u_i^n}{\partial y}\right| \ge 1 \end{cases} \tag{11}$$

- Convergence if $\Delta\lambda_i^n = \max\left|\lambda_i^n - \lambda_{i-1}^n\right| < \varepsilon_1$, where ε_1 is the tolerance for the Lagrange multiplier.
- $i = i + 1$

3. Stopping criterion.
4. $n = n + 1$.

Here r is an iterative parameter. The convergence of the above algorithm is proved in [9]. The choice of the stopping criterion will be discussed in the next section.

The present method is very convenient and easy to implement. In addition to providing the velocity and stress distributions at each time step, it also predicts the boundary separating yielded and unyielded zones. From the definition of λ (Eq. (8)), it can easily be observed that $|\lambda| = 1$ in the yielded regions and $|\lambda| < 1$ in the unyielded ones. The yield surface is defined as the isostress of $|\tau| = Bn$, i.e. at $|\lambda| = 1$. The evolution of the yield surface is of great importance in the present work.

3. Results and discussion

For the discretization of the one-dimensional domain, we use centered finite differences in space and the fully-implicit backward Euler scheme in time. The results presented in this work have been

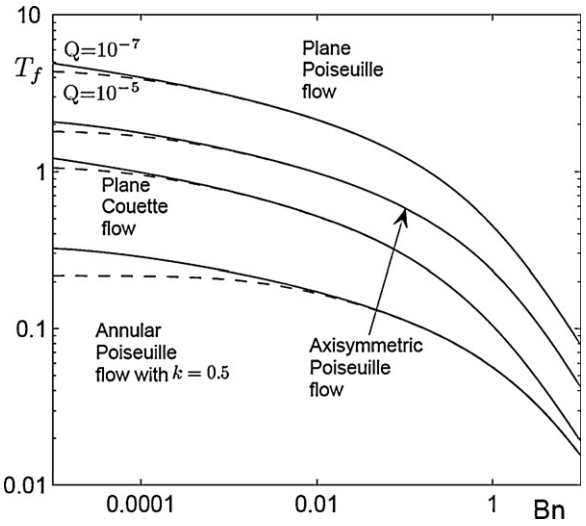

Fig. 1. Calculated stopping times for $Q = 10^{-5}$ (dashed lines) and 10^{-7} in cessation flows of a Bingham fluid: plane Couette, axisymmetric and plane Poiseuille flows; annular Poiseuille flow with $k = 0.5$. T_f is the finite stopping time defined in [1,2].

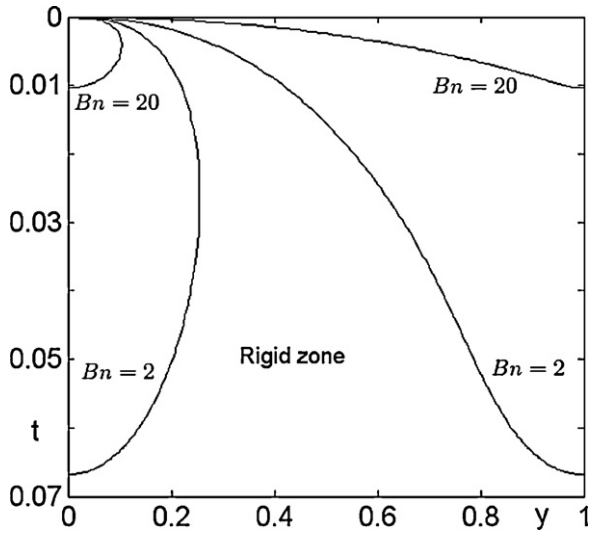

Fig. 2. Evolution of the yield surface in cessation of plane Couette flow of a Bingham fluid for $Bn = 2$ and $Bn = 20$.

obtained with 500 nodes. The effect of the time step has also been investigated; as the Bingham number is increased, faster transients are occurring and thus the time step should be reduced in order to ensure satisfactory accuracy. In general, the (dimensionless) time step ranged from 10^{-4} to 10^{-7}.

Another issue also raised by Chatzimina et al. [1,2] is the criterion used for calculating the numerical stopping time. Chatzimina et al. [1,2] presented results for two tolerances, i.e. values of the volumetric flow rate so low that the flow can be taken as practically stopped: $Q = 10^{-3}$ and 10^{-5}. The numerical stopping times for these two values of Q coincide for moderate or large Bingham numbers ($Bn \geq 0.1$). Chatzimina et al. [1,2] then presented results with the numerical stopping time as that required to reach $Q = 10^{-5}$. We have obtained analogous results for the two lower values of the volumetric flow rate, i.e., $Q = 10^{-5}$ and 10^{-7}. Fig. 1 shows plots of the calculated numerical stopping times versus the Bingham number for all cessation flows of interest. The results for $Q = 10^{-5}$ and 10^{-7} coincide in all flows for $Bn \geq 10^{-2}$ and differ for $Bn < 10^{-2}$, so for the small Bn numbers a more rigorous criterion should be applied. The current method produces a velocity approximation that contains regions of zero strain rate, and this provides a possibility to use the criterion $Q = 0$ for the stopping problems. So, in the remaining numerical experiments presented hereafter for the stopping problems, we have used the criterion $Q = 0$. Concerning the cases where the imposed pressure gradient is non-zero, as a stopping criterion we apply a tolerance such that $|Q^n - Q^{n-1}| < 10^{-7}$.

3.1. Plane Couette flow

The initial condition is the standard linear velocity profile. The lower plate which moves with unit velocity suddenly comes to rest at time $t = 0$. As a first test of the numerical code and the method, we reproduced the results of Chatzimina et al. [1], namely the evolution of the velocity profiles for $Bn = 0$ (Newtonian), 2 and 20. An interesting feature of the cessation of viscoplastic flows, not shown in Refs. [1] or [2], is the evolution of the interface between yielded and unyielded regions. This is shown in Fig. 2 for $Bn = 2$ and 20. The velocity inside the band is positive and at the two ends is equal to zero. Consequently, the velocity derivative $\partial u/\partial y$ changes sign at some point of this interval: therefore, this point belongs to a rigid zone. The present results confirm the theoretical analysis of Huilgol [27].

Fig. 3 shows the numerical stopping time T_f versus the Bingham number. The calculated curve is just below the theoretical upper bound provided by Huilgol et al. [4] for the whole range of Bn. This result indicates an advantage of the Lagrangian method over regularization methods. The corresponding results of Chatzimina et al. [1] with the Papanastasiou regularization of the Bingham model are satisfactory only for very low and for moderate to high Bingham numbers. For low to moderate Bingham numbers their numerical stopping times were actually above the upper bound because the regularization parameter was not sufficiently high. Using a higher value of the latter, however, would have led to very long computation times.

3.2. Plane Poiseuille flow

It is well known that steady-state Poiseuille flows of a Bingham fluid exist only if the applied pressure gradient exceeds a critical value. With our dimensionalization, this critical pressure gradient for plane Poiseuille flow is equal to the Bingham number, Bn. In the present time-dependent calculations, we start with a steady-state

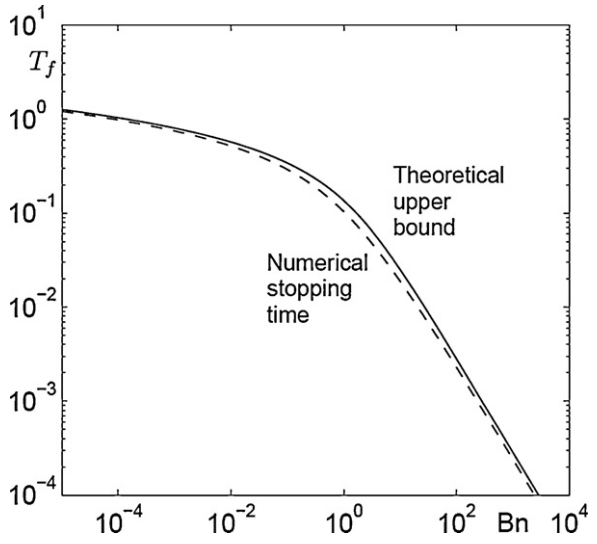

Fig. 3. Comparison of the computed stopping time ($Q = 10^{-7}$) in cessation of plane Couette flow of a Bingham fluid with the theoretical upper bound [3,4].

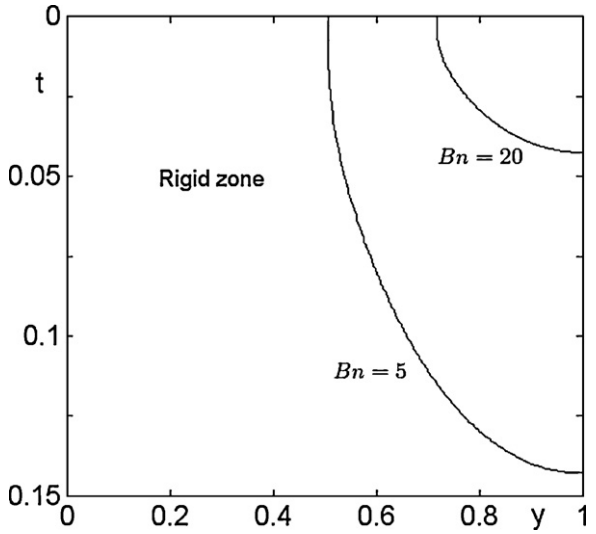

Fig. 4. Evolution of the yield surface in cessation of plane Poiseuille flow of a Bingham fluid for $Bn = 5$ and $Bn = 20$.

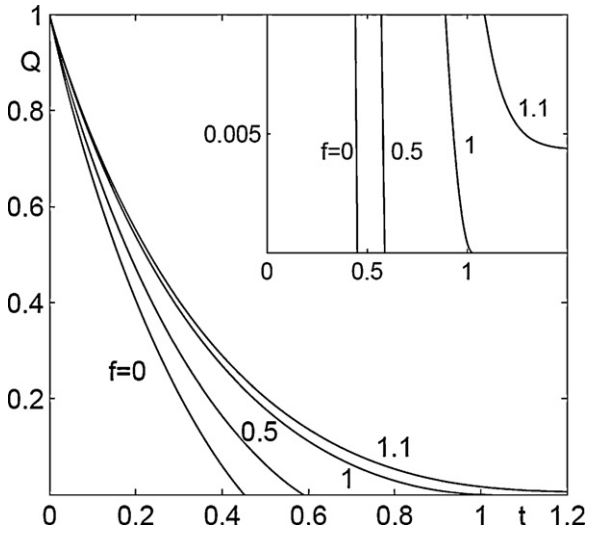

Fig. 6. Evolution of the volumetric flow rate in cessation of plane Poiseuille flow of a Bingham fluid with $Bn = 1$ and for various values of an imposed pressure gradient f (inset) detail showing that a finite volumetric flow rate is reached when $f > 1$.

solution corresponding to a pressure gradient $f_0 > Bn$ and at $t = 0$, the pressure is set to a new value f. If $f \leq Bn$, then the flow will eventually stop either at infinite (Newtonian) or finite (Bingham) time. If $f > Bn$, the flow does not stop; another (non-zero) steady-state is reached instead, with the volumetric flow rate corresponding to the new pressure gradient.

We have again repeated the calculations of Chatzimina et al. [1] and obtained essentially the same results. Fig. 4 shows the evolution of the interface between yielded and unyielded regions for $Bn = 5$ and 20. As expected, the size of the unyielded region increases with time and with the Bingham number. The numerical stopping time for the case of $f = 0$ (i.e., when the imposed pressure gradient is set to 0, cf. Fig. 16 of [1]) is plotted as a function of Bn in Fig. 5. Again, the computed stopping times are just below the theoretical upper bound [3,4] for the whole range of Bn numbers; for low to moderate Bingham numbers, in particular, they are more accurate than the regularization results of Chatzimina et al. [1].

As pointed out by Chatzimina et al. [1], an important difference between the predictions of the ideal and the regularized Bingham model is revealed when the imposed pressure gradient is non-zero

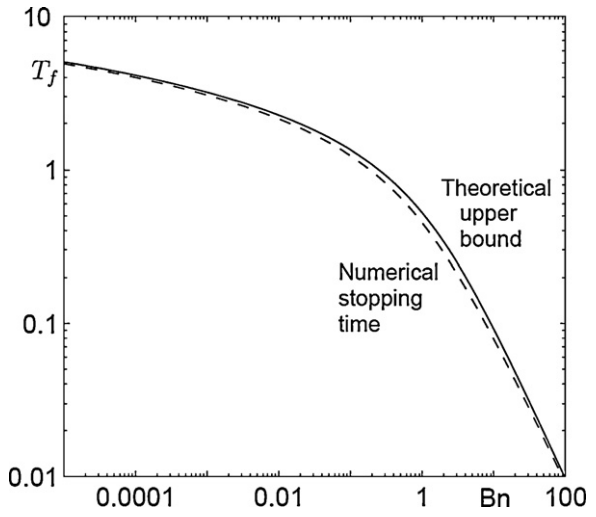

Fig. 5. Comparison of the computed stopping time ($Q = 10^{-7}$) in cessation of plane Poiseuille flow of a Bingham fluid with the theoretical upper bound [3,4] for $f = 0$ (zero pressure gradient).

($f \neq 0$) and below the critical value Bn at which a non-zero steady-state Poiseuille solution exists. In order to make comparisons with their results, we carried out simulations for $Bn = 1$ and different values of f. The evolution of the volumetric flow rate is shown in Fig. 6. As expected, for $f = 0$, 0.5 and 1, the flow stops while for $f = 1.1$, it evolves to a new steady regime. The inset of Fig. 6 is a zoom showing these effects in detail. It should be noted that in [1], the flow does not stop when $f = 0.5$ and 1, but a new steady-state is reached with a very small but non-zero-velocity corresponding to a small but non-zero volumetric flow rate. As pointed out by Chatzimina et al. [1], the value of the latter may be reduced by increasing the value of the regularization parameter, but it will always be non-zero. This effect is a direct consequence of the regularization of the Bingham model; the regularized model does not correspond to an ideal viscoplastic material but to a highly viscous fluid for very low strain rates.

3.3. Axisymmetric Poiseuille flow

The results for the axisymmetric Poiseuille flow reveal some subtle but very interesting differences from their planar counterparts. In Fig. 7 we show the evolution of the velocity profile for $Bn = 1$. The inset of Fig. 7 is a zoom near the wall, which shows that a second unyielded region of a smaller size appears near the wall, where the fluid velocity is zero. This effect (a wall static layer) was also noted in [1] for a higher value of the Bingham number. Chatzimina et al. [1] stated that "the growth of this region cannot be explained physically and is considered as a numerical artifact due to regularization of the constitutive equation". The current computations based on the Lagrangian method show convincingly that this effect takes place for all Bingham numbers. The dead zone appears shortly before cessation and grows very quickly. Therefore, this is not a numerical artifact caused by the regularization, but an inherent feature of the Bingham model for this type of flow. This phenomenon is more clearly illustrated in Fig. 8, where we show the evolution of the yield surface for $Bn = 1$, 2, 5, 10 and 20. The stars on these graphs designate the point at which the plug region and the zero-velocity region meet. The size of the latter region decreases with increasing Bingham number.

As in all flows studied, the numerical stopping times for $f = 0$, plotted versus Bn in Fig. 9, agree very well with the theoretical upper bounds [3,4]. For the circular Poiseuille flow we also consider

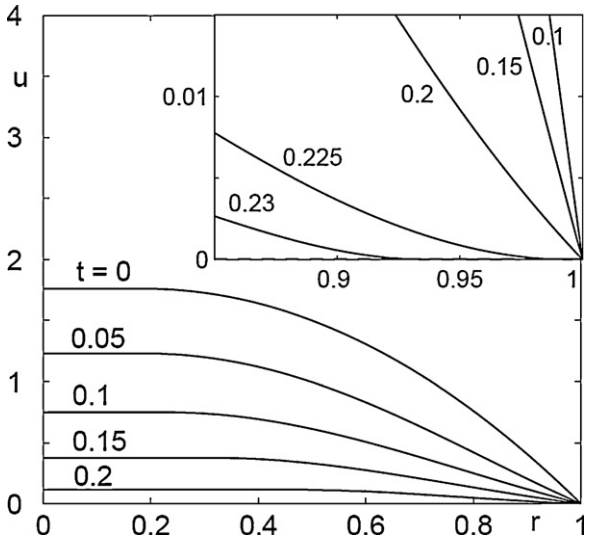

Fig. 7. Evolution of the velocity profile in cessation of axisymmetric Poiseuille flow of a Bingham fluid with $Bn = 1$ (inset) detail near the wall.

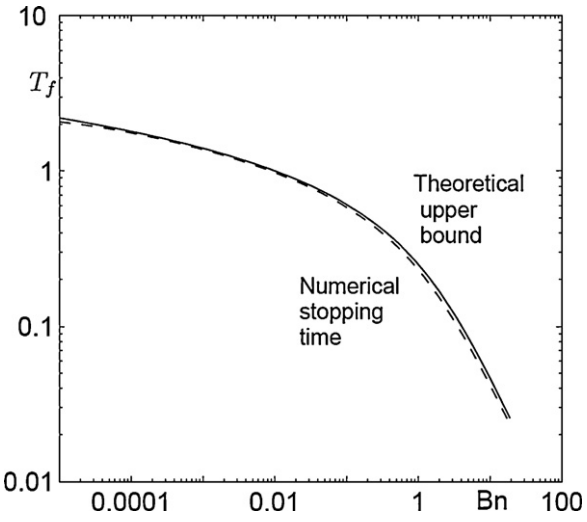

Fig. 9. Comparison of the computed stopping time ($Q = 10^{-7}$) in cessation of axisymmetric Poiseuille flow of a Bingham fluid with the theoretical upper bound [3,4] for $f = 0$ (zero pressure gradient).

the case where the imposed pressure gradient is non-zero but less than the critical value, which in this case is equal to $2Bn$. The evolution of the yield surface for $Bn = 2$ and various values of the imposed pressure gradient below and above the critical value ($f_{crit} = 4$) is shown in Fig. 10. The most interesting result is the presence of the second unyielded region, which depends on the pressure gradient. For $f = 0$, 0.5, and 1, the dead zone appears near the wall. For $f = 1.5$, 2, and 4, there are no dead zones, and the size of the plug region increases until it fills the whole pipe. For $f = 6$, the flow reaches the new steady regime, as expected, and the size of the plug region becomes constant.

3.4. Annular Poiseuille flow

Our simulations of the cessation of annular Poiseuille flow were in very good agreement with the results of Chatzimina et al. [2]. When the value of the diameter ratio is quite small (e.g., $k = 0.1$), the flow is quite similar to the circular Poiseuille flow. In particular, our simulations revealed the appearance of the dead zone near the outer wall (wall static layer). It is not difficult to mathematically argue (based on the governing differential equations and considering the signs of each term) that this is not the case for the inner wall. The same arguments, when applied to the plane Poiseuille flow, show no emergence of a dead zone near the wall, while this is possible for the axisymmetric Poiseuille flow. For $k = 0.5$, no dead zones have been observed. The evolution of the yield surfaces with $Bn = 20$ and $k = 0.1$, 0.2, 0.3 and 0.5 is depicted in Fig. 11. One may observe that the size of dead zone decreases with increasing the value of k. The numerical stopping times for $k = 0.1$ and 0.5 are compared with the theoretical upper bounds [3] in Fig. 12. Again the numerical results satisfy the theoretical predictions for the whole range of Bingham numbers.

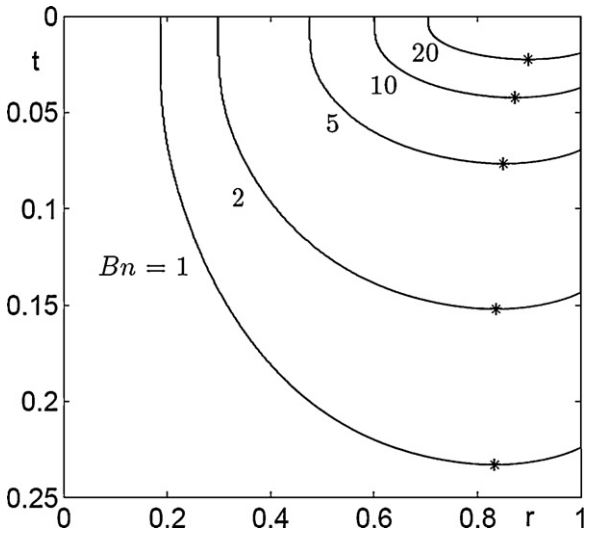

Fig. 8. Evolution of the yield surface in cessation of axisymmetric Poiseuille flow of a Bingham fluid for various Bingham numbers. The stars (*) denote the points at which the plug region and the zero-velocity region meet.

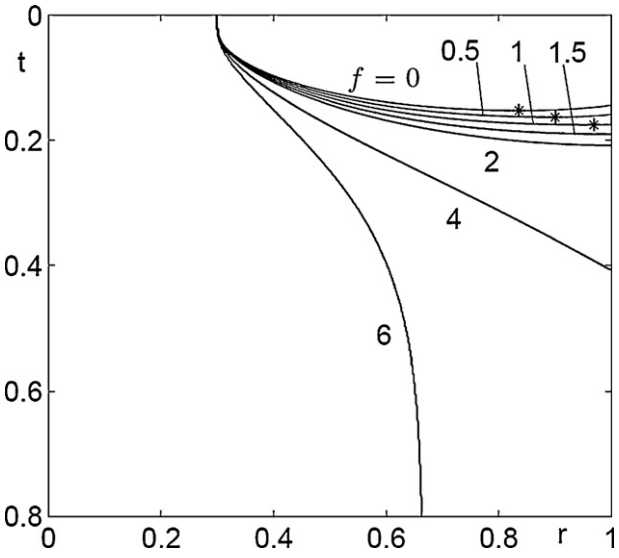

Fig. 10. Evolution of the yield surface in cessation of axisymmetric Poiseuille flow of a Bingham fluid with $Bn = 2$ for various values of the imposed pressure gradient f. The stars (*) denote the points at which the plug region and the zero-velocity region meet.

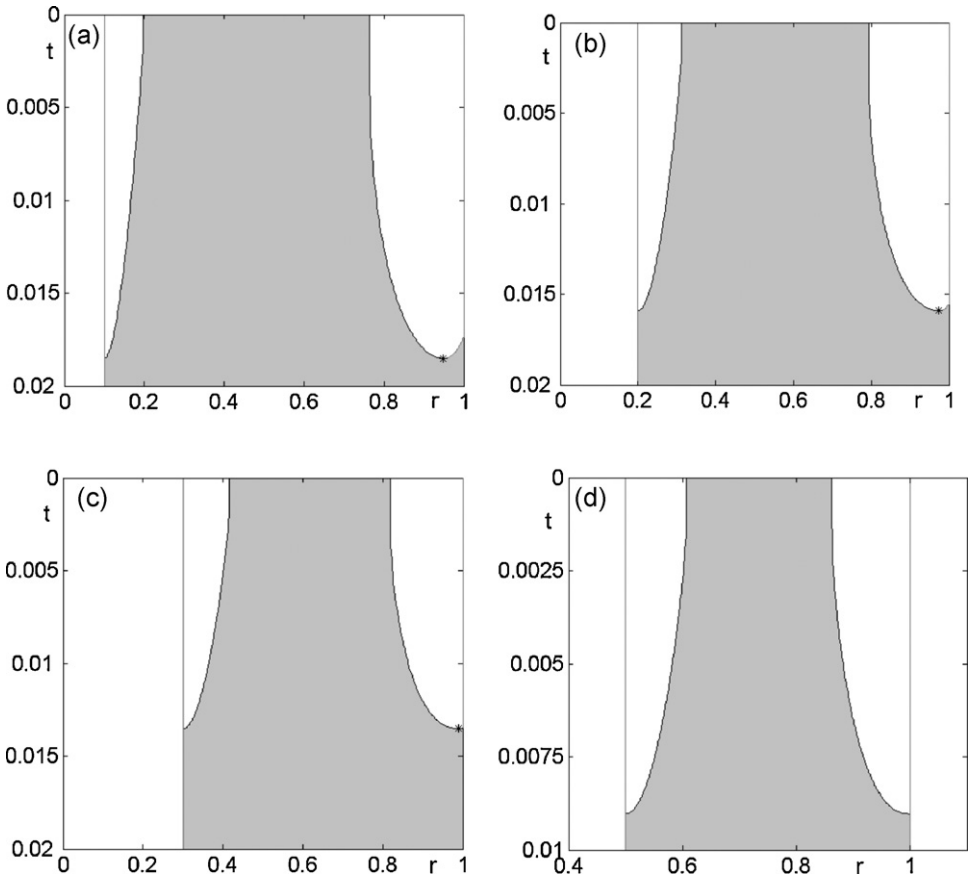

Fig. 11. Evolution of the yield surface in cessation of annular Poiseuille flow of a Bingham fluid with $Bn = 20$ and different radii ratios: (a) $k = 0.1$; (b) $k = 0.2$; (c) $k = 0.3$; and (d) $k = 0.5$. The stars (*) denote the points at which the plug region and the zero-velocity region meet.

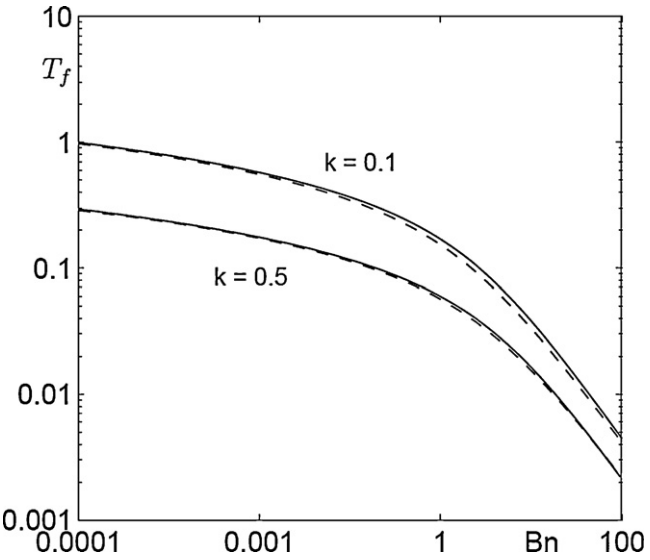

Fig. 12. Comparison of the computed stopping times (dashed lines obtained with $Q = 10^{-7}$) with the theoretical upper bounds (solid lines) [2] for $k = 0.1$ and $k = 0.5$, in cessation of annular Poiseuille flow of a Bingham fluid.

4. Conclusions

We have used the Lagrangian method to solve benchmark, one-dimensional cessation flows of an ideal Bingham plastic. Comparisons have been made with the analytical upper bounds for the stopping times [3,4] and the numerical results of Chatzimina et al. [1,2], who used the regularized Papanastasiou model. Compared to the latter method, the Lagrangian method yields superior results regarding the location of the yield surface and the behavior of the ideal Bingham model in extreme situations (for example, low *Bn* number flows). The finite stopping times are always slightly below the well known theoretical bounds for all *Bn* ranges. The unyielded surfaces are more conservative than the ones obtained with the regularized models, which need a very high regularization parameter to approach the ideal Bingham model, especially at low and moderate Bingham numbers. This became obvious in cessation of axisymmetric and annular Poiseuille flows, when a dead region near the solid wall (wall static layer) was found for all *Bn* numbers. The regularized model gave such regions only over a certain range of *Bn* ($\geq$20).

On the other hand, the results of the regularized model are shown to stand the test against the more rigorous and conservative current results, as the differences are not that great. The results with the Papanastasiou model are easily obtainable with any viscous code by writing a simple viscosity subroutine, and can be had very fast with modern computers. They are ideal for engineering calculations and for giving a very good *approximation* to the ideal Bingham model. Perhaps they are better in representing real materials, where discontinuities may not be justified.

The present results are offered as reference solutions for researchers working with the numerical simulation of viscoplasticity. They are the prelude for more demanding two- and three-dimensional simulations, which are currently in progress.

Acknowledgements

Financial support from the program "SOCRATES" for scientific exchanges between Greece and Cyprus is gratefully acknowledged. The research was also partially supported by RFBR grants 08-01-00353a, 09-01-00565a. The reviewers are also thanked for their useful comments and suggestions.

References

[1] M. Chatzimina, G.C. Georgiou, I. Argyropaidas, E. Mitsoulis, R.R. Huilgol, Cessation of Couette and Poiseuille flows of a Bingham plastic and finite stopping times, J. Non-Newtonian Fluid Mech. 129 (2005) 117–127.
[2] M. Chatzimina, C. Xenofontos, G.C. Georgiou, I. Argyropaidas, E. Mitsoulis, Cessation of annular Poiseuille flows of Bingham plastics, J. Non-Newtonian Fluid Mech. 142 (2007) 135–142.
[3] R. Glowinski, Numerical Methods for Nonlinear Variational Problems, Springer-Verlag, New York, 1984.
[4] R.R. Huilgol, B. Mena, J.M. Piau, Finite stopping time problems and rheometry of Bingham fluids, J. Non-Newtonian Fluid Mech. 102 (2002) 97–107.
[5] T.C. Papanastasiou, Flow of materials with yield, J. Rheol. 31 (1987) 385–404.
[6] E. Mitsoulis, Annular extrudate swell of pseudoplastic and viscoplastic fluids, J. Non-Newtonian Fluid Mech. 141 (2007) 138–147.
[7] I.A. Frigaard, C. Nouar, On the usage of viscosity regularisation methods for visco-plastic fluid flow computation, J. Non-Newtonian Fluid Mech. 127 (2005) 1–26.
[8] G. Duvaut, J.L. Lions, Inequalities in Mechanics and Physics, Springer-Verlag, Berlin, 1976.
[9] R. Glowinski, J.L. Lions, R. Tremolieres, Numerical Analysis of Variational Inequalities, North-Holland, Amsterdam, 1981.
[10] E.J. Dean, R. Glowinski, G. Guidoboni, On the numerical simulation of Bingham visco-plastic flow: old and new results, J. Non-Newtonian Fluid Mech. 142 (2007) 36–62.
[11] E.J. Dean, R. Glowinski, Operator-splitting methods for the simulation of Bingham visco-plastic flow, Chin. Ann. Math. 23 (2002) 187–204.
[12] Z. Yu, A. Wachs, A fictitious domain method for dynamic simulation of particle sedimentation in Bingham fluids, J. Non-Newtonian Fluid Mech. 145 (2007) 78–91.
[13] L.V. Muravleva, E.A. Muravleva, Uzawa method on semi-staggered grids for unsteady Bingham media flows, Russ. J. Numer. Anal. Math. Model. 24 (2009) 543–563.
[14] M. Fortin, R. Glowinski, Augmented Lagrangian Methods: Application to the Numerical Solution of Boundary-Value Problems, North Holland, Amsterdam, 1983.
[15] R.R. Huilgol, M.P. Panizza, On the determination of the plug flow region in Bingham fluids through the application of variational inequalities, J. Non-Newtonian Fluid Mech. 58 (1995) 207–217.
[16] Y. Wang, Finite element analysis of the duct flow of Bingham plastic fluids: an application of the variational inequality, Int. J. Numer. Methods Fluids 25 (1997) 1025–1042.
[17] N. Roquet, P. Saramito, An adaptive finite element method for viscoplastic fluid flows in pipes, Comput. Methods Appl. Mech. Eng. 190 (2001) 5391–5412.
[18] M.A. Moyers-Gonzalez, I.A. Frigaard, Numerical solution of duct flows of multiple visco-plastic fluids, J. Non-Newtonian Fluid Mech. 122 (2004) 227–241.
[19] R.R. Huilgol, Z. You, Application of the augmented Lagrangian method to steady pipe flows of Bingham, Casson and Herschel–Bulkley fluids, J. Non-Newtonian Fluid Mech. 128 (2005) 126–143.
[20] A. Wachs, Numerical simulation of steady Bingham flow through an eccentric annular cross-section by distributed Lagrange multipliers/fictitious domain and augmented Lagrangian methods, J. Non-Newtonian Fluid Mech. 142 (2007) 183–198.
[21] E.A. Muravleva, Finite-difference schemes for the computation of viscoplastic medium flows in a channel, Math. Models Comp. Simul. 1 (2009) 768–779.
[22] J.C. De los Reyes, S. Gonzàlez, Path following methods for steady laminar Bingham flow in cylindrical pipes, ESAIM: Math. Model. Numer. Anal. 43 (2009) 81–117.
[23] N. Roquet, P. Saramito, An adaptive finite element method for Bingham fluid flows around a cylinder, Comput. Methods Appl. Mech. Eng. 192 (2003) 3317–3341.
[24] G. Vinay, A. Wachs, J.-F. Agassant, Numerical simulation of non-isothermal viscoplastic waxy crude oil flows, J. Non-Newtonian Fluid Mech. 128 (2005) 144–162.
[25] A. Wachs, G. Vinay, I. Frigaard, A 1.5 numerical model for the start up of weakly compressible flow of a viscoplastic and thixotropic fluid in pipelines, J. Non-Newtonian Fluid Mech. 159 (2009) 81–94.
[26] P.P. Mosolov, V.P. Myasnikov, Variational methods in the theory of the fluidity of a viscous–plastic medium, PMM 29 (1965) 468–492.
[27] R.R. Huilgol, On kinematic conditions affecting the existence and nonexistence of a moving yield surface in unsteady unidirectional flows of Bingham fluids, J. Non-Newtonian Fluid Mech. 123 (2004) 215–221.